

Nonlinear Strain Stiffening is Not Sufficient to Explain How Far Cells Can feel on Fibrous Protein Gels

Mathilda S. Rudnicki, Heather A. Cirka, Maziar Aghvami, Edward A. Sander, Qi Wen, and Kristen L. Billiar

Supporting Material

Analysis of fiber reorganization in confocal reflectance images

Non-uniform intensity profiles along the gel surface

The distance a cell reorganizes the fibers along the surface of a gel was determined by analyzing intensity profiles using ImageJ. Average grayscale values were plotted against distance for 100 pixel-wide regions (as shown by red rectangles in Fig. S1 A) fit to polynomial curves. The distance from the cell edge where the grayscale value was indistinguishable from noise (as determined by the intersection of baseline value curve with the data curve), is interpreted as the location where the cell tractions no longer visibly reorganize the matrix. Example average intensity profiles are shown in Fig. S1.

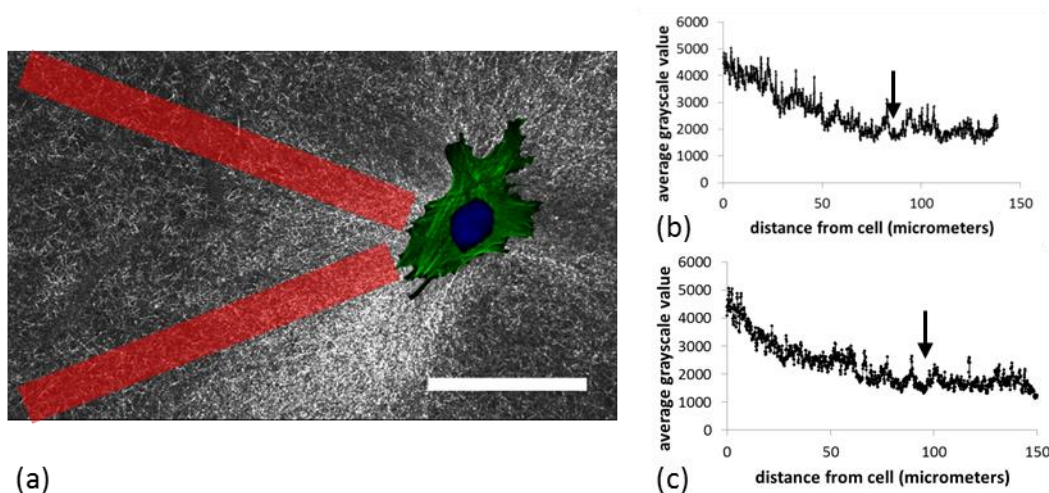


Fig. S1 (a) Representative confocal reflectance image of a collagen gel (stitched from multiple images) overlaid with confocal image of fluorescently stained cell and example regions of analysis in red. (b and c) Examples of average grayscale versus distance plots for 100 pixel-wide regions of a confocal reflectance image; arrows indicate extent of fiber reorganization from edge of cell located. (Scale bar = 75 μm).

Skewing of intensity distribution below cells

In our analysis of how deeply into the gel cells affect the fibrous structure, normal probability plots were used to determine the normality of grayscale intensity values in a region of interest of confocal reflectance images. The normal probability plot is a graphical technique used to determine the extent to which a data distribution is Gaussian. In this method, the probability versus error data are plotted (where error in this case is the difference from the average intensity) and the degree to which the plot follows a straight line indicates how well the data can be represented by a Gaussian distribution. Far from a cell and in acellular gels (Fig. S2 A), we empirically found that the normal probability plot was linear for ~80% of the data (see Fig. S2 B). When the cell remodels the matrix, it creates fiber densifications which skew the

grayscale values in the region of interest towards higher values (Fig. S2 C), creating a non-normal distribution (Fig. S2 D).

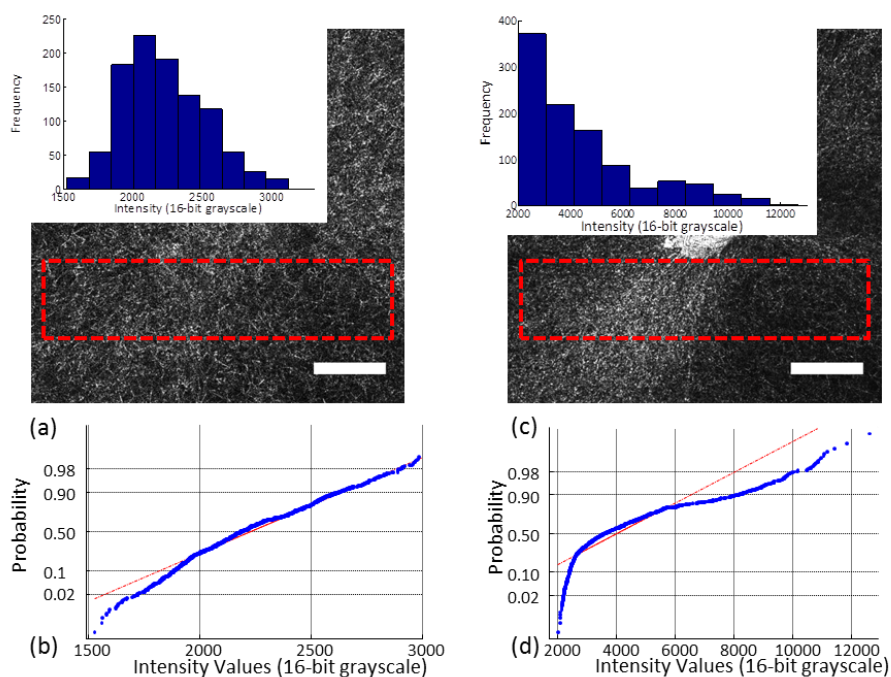


Fig. S2 Confocal reflectance mode images of 4 mg/ml collagen gel 7.5 μm below cell (a) and at the surface (b). Histograms of intensity (16-bit grayscale) versus distance are shown (insets) for regions of analysis indicated by red rectangles. Probability plots in (c) and (d) correspond to analysis regions in (a) and (b), respectively. Far from the cell, 80% of the data fall along a line indicating a roughly Gaussian distribution of intensities and no measurable effects of the cell on the fiber reflectance pattern (as shown in (b)), whereas cell reorganization of the fibrous matrix at the surface skews the intensity distribution and yielding non-normally distributed data (as shown in (d)).

Details on the development of the continuum finite element model

Validation of linearly elastic model results

A radially-symmetric continuum finite element (FE) model of a cell exerting inward traction on the surface on a finite thickness gel, as shown in Fig. S3 A and B, was developed based on work by Sen et al.(1), Mehrotra et al. (2), and Munevar et al. (3).

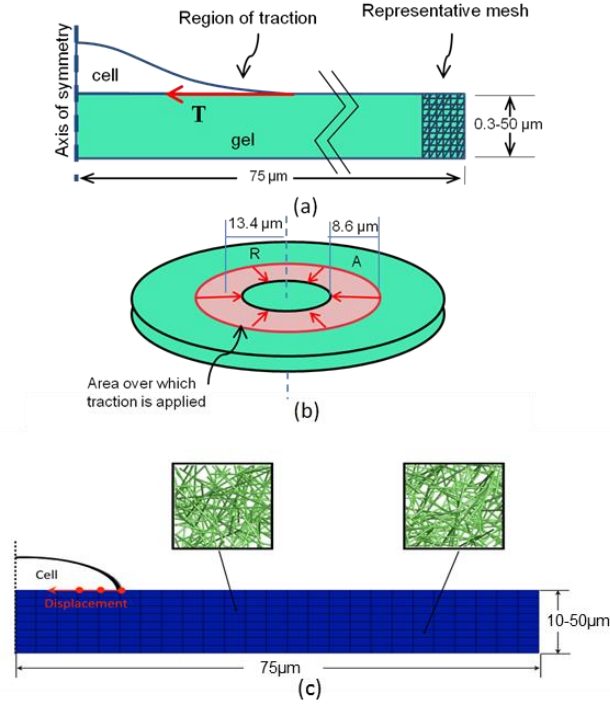


Fig. S3: (a) Schematic of the continuum finite element model. Traction is applied to the free top surface of a radially symmetric substrate; the lower boundary is fixed and the left boundary can move only vertically. Nine versions of the model were created in different thicknesses from 0.3-50 μm. The cell is shown for reference but is not modeled. (b) Revolved about the axis, the model simulates a round cell applying traction along an annulus of dimensions provided in the schematic. (c) Schematic of the 10 μm-thick fiber-based finite element model with simplified thin rectangular geometry which is one element deep (4 μm). Displacement is applied to the nodes on the top surface; the lower boundary is fixed, the left boundary can move only vertically, and the front and back surfaces are restrained in the z-direction (into the page). Three versions of the model were created in different thicknesses (10, 30, and 50 μm) with 200 different types of (initially) isotropic fiber distributions (two examples are shown in the figure).

Degree of strain stiffening of nonlinear material model

The fibrin gel rheometry data from Winer et al. (4) were fit to a third-order reduced polynomial model in ABAQUS with the following form:

$$W = C_{10}(I_I - 3) + C_{10}(I_I - 3)^2 + C_{10}(I_I - 3)^3 + \frac{1}{D_1} \quad (\text{S1})$$

where W is the strain energy per unit volume, I_I is the first strain invariant, and D_1 is a compressibility term. The material model was validated by simulating the simple shear experiment using rectangular FE models and comparing the shear stress v. shear strain output with the experimental data (see Fig. S4 A).

In an effort to determine the effect of the extent of nonlinearity of the material on substrate displacement, the data from Winer et al. (4) were made “more nonlinear” by increasing the “toe region” of the stress-strain behavior i.e., the strain-stiffening behavior appears at a higher strain as shown in Fig. S4 B. The material model has little effect on the normalized displacement-thickness relationship, as shown in Fig. S4 C. As the thickness is increased past 20 μm the model becomes unstable and was not used further.

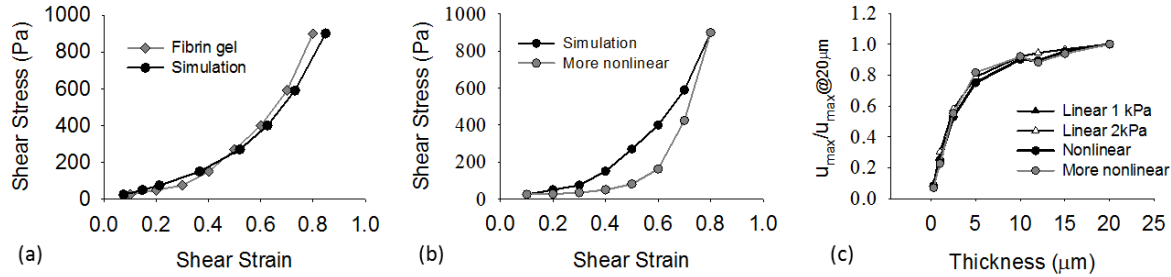


Fig S4: (a) The results of the simple shear simulations are compared with the original rheometry data from Winer et al. (12) to ensure that the fibrin gel material responds as intended. (b) The nonlinear material is modified to show stiffening at higher strains. (c) The relationship between substrate thickness and normalized peak displacement values for 1 kPa and 2 kPa linear gels and for the “nonlinear” and “more nonlinear” material models from the FE analysis are qualitatively indistinguishable. Quantitatively, the “nonlinear” material responds similar to the 2 kPa linear gel for thicknesses over 5 μm ; the “more nonlinear” material responds much like a 1kPa gel, but the simulations become unstable at $h > 20 \mu\text{m}$ and was not used for further simulations.

Comparison of displacement vs. thickness for the continuum model

The strain distributions for the linearly elastic model are similar to those published by Sen et al. (1), although the peak strains occur at the inner edge of the applied traction in our model and closer to the cell edge in the previous model. Due to differences in the location of the applied cell traction and definitions of displacement (maximum v. average), our surface displacement v. substrate thickness results are not identical to the published values, yet the results from the two models match closely when normalized to the displacement of the thickest material at each substrate stiffness level. When normalized, the data from each of the four different substrates stiffness levels ($E = 1, 5, 12,$ and 40 kPa) from our model lie roughly on top of those from the previous model (Fig. S5). The normalized displacements from all four stiffness levels of the present model collapse onto a single curve since the system is linear and there is no effect of the cell’s stiffness in parallel to the gel.

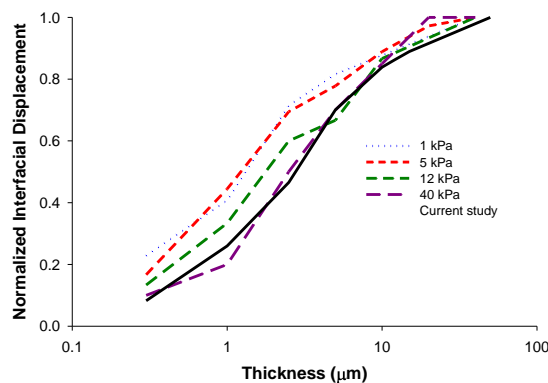


Fig S5: Maximum interfacial (surface) displacement predicted from the FE model (in the -x direction) for 500 Pa applied traction as a function of gel thickness, normalized to the value for the “infinitely” thick (50 μm) gel case (solid black line). The normalized displacements from all four stiffness levels of the present model collapse onto the black line since the system is linear. The mean interfacial displacements reported by Discher and colleagues (Figure 4d in Sen et al. (1)), normalized to the value for the “infinitely” thick (50 μm) gel case, are plotted for comparison. Although there are moderate differences in absolute values of reported displacement, the agreement between our model results and those of Sen et al. (1) demonstrates that the functional form of the effect of gel thickness on surface displacement is the same regardless of method of loading (cell prestress v. uniform annulus of traction), radial location of traction, and use of mean v. maximum displacement between our analyses.

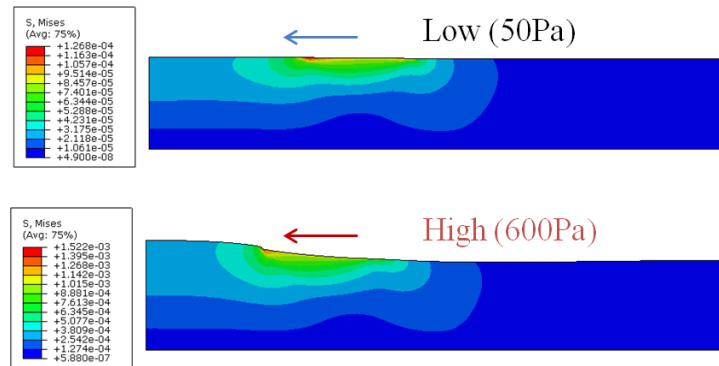
Table S1: Tabulated data of maximum surface displacement of the FE model for linearly elastic gels of various linear stiffness levels due to 500Pa applied traction

Thickness (μm)	Gel Stiffness (kPa)			
	1	5	12	40
0.3	0.434	0.0869	0.0362	0.0109
1	1.41	0.282	0.118	0.0353
2.5	2.74	0.548	0.228	0.0685
5	3.79	0.758	0.316	0.0947
10	4.53	0.906	0.377	0.113
12	4.65	0.930	0.388	0.116
15	4.79	0.957	0.399	0.120
20	4.97	0.994	0.414	0.124
50	5.42	1.08	0.452	0.136

Magnitude and location of application of traction

Changing level of traction

In terms of the magnitude of applied traction, we chose 50 to 600 Pa (Fig. S6 and Fig. S7) which is in the range of published traction stresses near the edge of a cell and which produces u_{max} values that roughly match measured surface displacements (generally 0.1 to 10 μm). Cell traction forces measured using standard 2D traction force microscopy (TFM) indicate that the traction applied by a cell covers a wide range of values, from up to 250 Pa for human tendon fibroblasts (5) to up to 36 kPa in 3T3 fibroblasts (3) and 430-750 Pa for BAECs (6). Neither our model nor previous models account for the increase in cell traction and spread area with substrate stiffness that is observed in many experimental studies (e.g., 7, 8).

**Fig. S6:** FE stress distribution results of cell-applied traction on 10 μm linear material (1 kPa). Note the similarity of the contour plots, but the difference in material deformation (deformation scale factor=1).

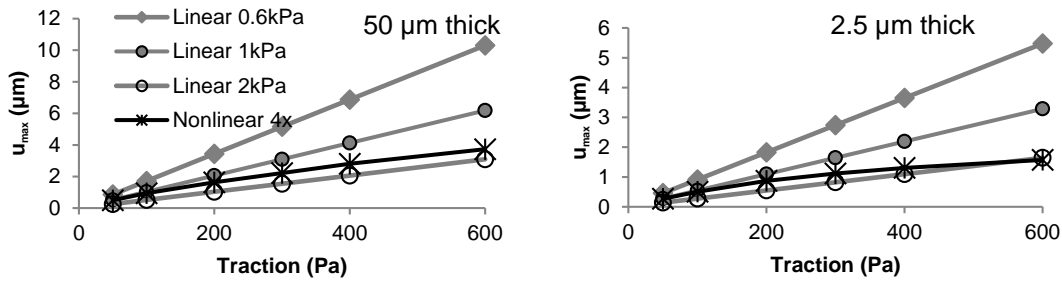


Fig. S7: The maximum displacement of the top surface of linear substrates increases linearly as traction is increased. However, the nonlinear material exhibits strain-stiffening behavior; as traction increases, the ability of the nonlinear material to deform is reduced. This strain-stiffening effect is amplified by decreasing the substrate thickness from 50 μm (a) to 2.5 μm (b). On the thin substrate, the gels deform to a lesser extent than the thick gels due to the impact of the rigid boundary under the substrate.

Changing size and location of cell-applied traction

The defined area of cell-gel interaction is specified by Mehrotra et al. (2) with two parameters: focal adhesion radius and width of the traction region. When the radius (R) is increased (i.e., a larger cell) or the traction region increases (i.e., more focal adhesions), the maximum surface displacement is increased. Changing the size of the cell or the size of the cell-applied traction surface also affects the effective stiffness of a linear material as shown in Fig. S8 A. An increase in R increases the effective stiffness, while an increase in A decreases the effective stiffness. These simulations are performed on a linear elastic substrate to focus on effects of cell geometry.

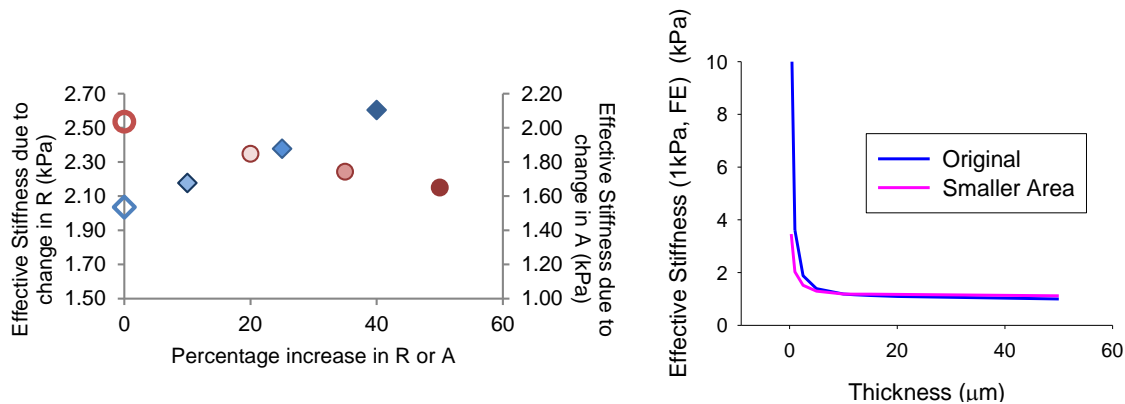


Fig. S8: a) The effective stiffness of a linear material is dependent on the dimensions of the applied traction, and thus on the geometry of the cell. Increasing the size of the cell (R , diamonds) increases the effective stiffness of the substrate. Conversely, increasing the size of the traction surface (A , circles) decreases the substrate effective stiffness. b) With the same force but a smaller area for the cell applied traction (traction \times area = constant), the linear material responds similarly to the original traction area, in terms of effective stiffness.

The above changes in R and A are performed with a constant traction (100 Pa). Due to the linearity of the material, the value of the applied traction will not affect the overall response of the material. To investigate the effective stiffness response of a cell that applies the same force but only at the very edge of the cell, the model was modified to include a smaller area of cell-applied traction and a higher traction to maintain the same force as 100 Pa over the original area. As shown in Fig. 8 B, the effective stiffness of the material with this smaller area follows the same shape as that with the original area.

Definition of surface displacement: u_{\max} vs. u_{avg}

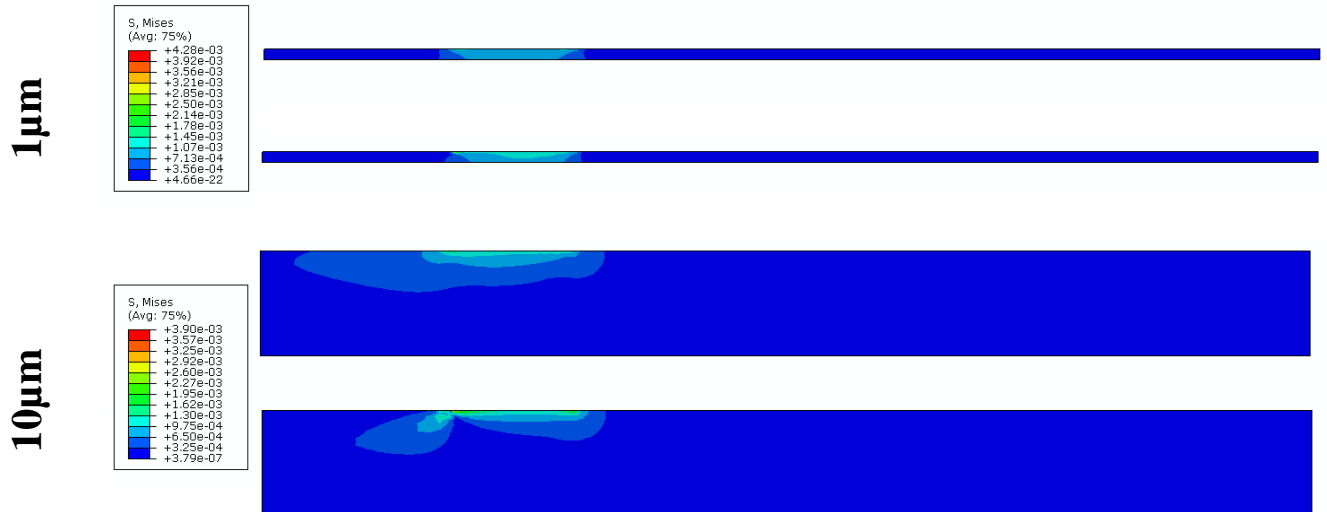
It is not known what physical cues (displacements, forces, strain energy, etc.) a cell senses which causes/allows it to spread more on a stiff surface than compliant one. For a given cell-generated traction, it is reasonable to assume that the resulting surface displacement provides an indication of the stiffness of a surface to the cell, with larger displacement on soft substrates and lower displacements on stiff substrates. Sen et al. (1) utilize the mean interfacial deformation, u_{avg} , as a representation of the work done by the cell on the matrix to compare between gel stiffness and thickness levels. In the present study, we utilize the maximum interfacial displacement u_{\max} , as a metric of the cells' ability to deform the matrix for a given traction, T , applied at a given location, R . We then calculate E_{eff} using these parameters (u_{\max} , T , R). u_{\max} is simpler to extract from the FE output, and is roughly linearly related to u_{avg} . To demonstrate this relationship, sample displacement data were collected at nodes along the top of the substrate where traction is applied for the following thicknesses: 0.3, 1, 2.5, 5, 10, 12, 15, 20, and 50 μm , as well as for the following substrate stiffnesses: 1, 5, 12, and 40 kPa. $u_{\max}:u_{\text{avg}} = 1.12 \pm 0.01 \mu\text{m}$ and ranged from 1.05 (on the thinnest gels 0.3 μm) to 1.19 (on a 1 μm thin gel).

Stiffness gradient

Using sloped gels allows the simultaneous analysis of many cells' responses to different thickness gels but also creates a gradient in effective stiffness. Strong stiffness gradients (2 and 4 kPa/100 μm) in PA gels have been shown to increase in directional motility and cell orientation relative to non-gradient controls (9). For our study, the slope ($\Delta h/\Delta x$) of the gel was chosen to be as low as practical ($\sim 10 \mu\text{m}/\text{mm}$) with thicknesses ranging from 0 to 300 μm (thickness of a two standard coverslips). When combined with the effective stiffness predictions from the FE model for the nonlinear material with an applied traction of 400 Pa, the gradient in stiffness is 0.02 kPa/100 μm in the 10-50 μm thickness range. Thus our predicted gradient appears to be too low to play a role in the cell response on our substrates.

Stress and strain distributions

Comparison of von Mises stress and strain distribution in linear and nonlinear gels were completed for many thickness levels (1, 10, 50 μm shown in Fig. S9 and Fig. S10, respectively) with traction applied at top surface of 600Pa. All distributions are plotted on undeformed geometry.



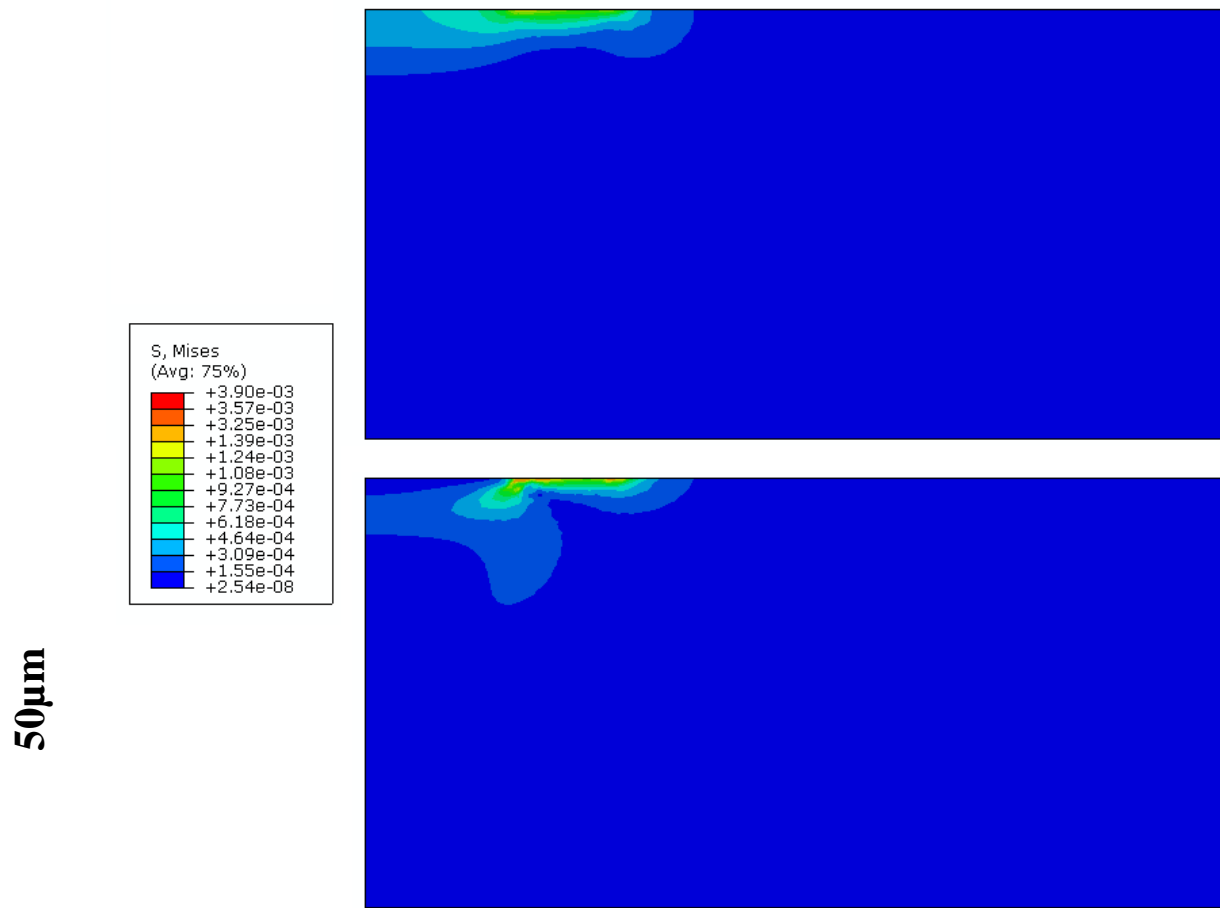
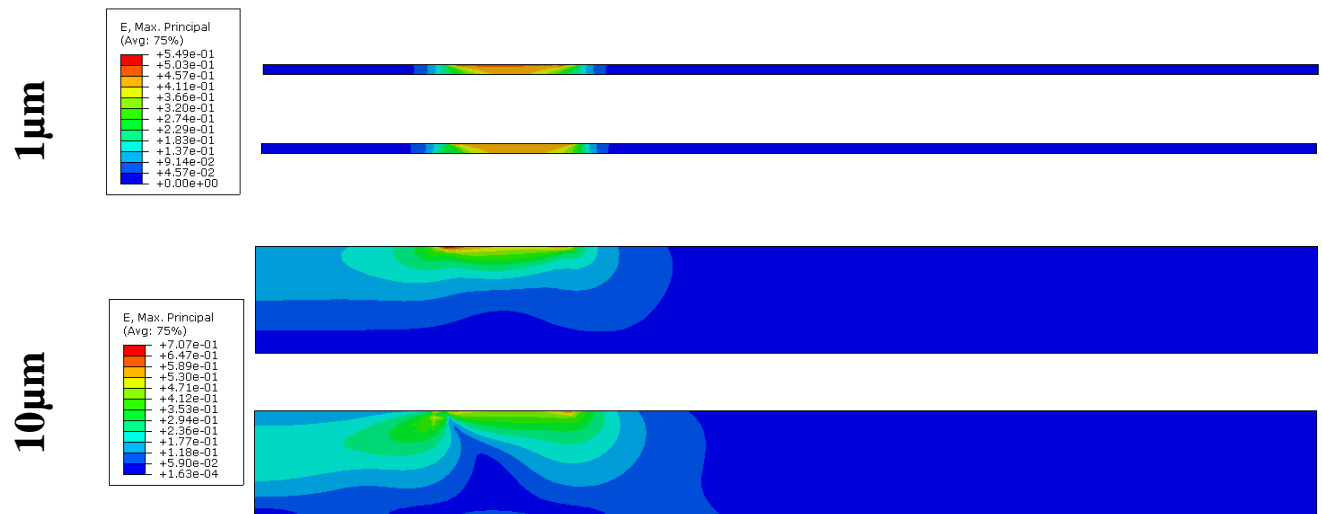


Fig. S9: Stress distributions for linear (above, 2kPa) and nonlinear (below, fibrin) gels of 1, 10, and 50 µm thickness, top to bottom with an applied traction of 500 Pa. The color scale is normalized to the maximum and minimum stresses in each case to show the stress profiles regardless of magnitude (deformation scale factor=0). The stress magnitudes for a given thickness are the same regardless of stiffness as expected for linear materials under traction loading (i.e., Boussinesq solution). The stress profiles extend less far into the strain-stiffening material compared to the linear material as can be seen by the distances both laterally and horizontally to the lowest contour, representing roughly 9% of the maximum stress. The stress contours are blunted in the strain-stiffening material.



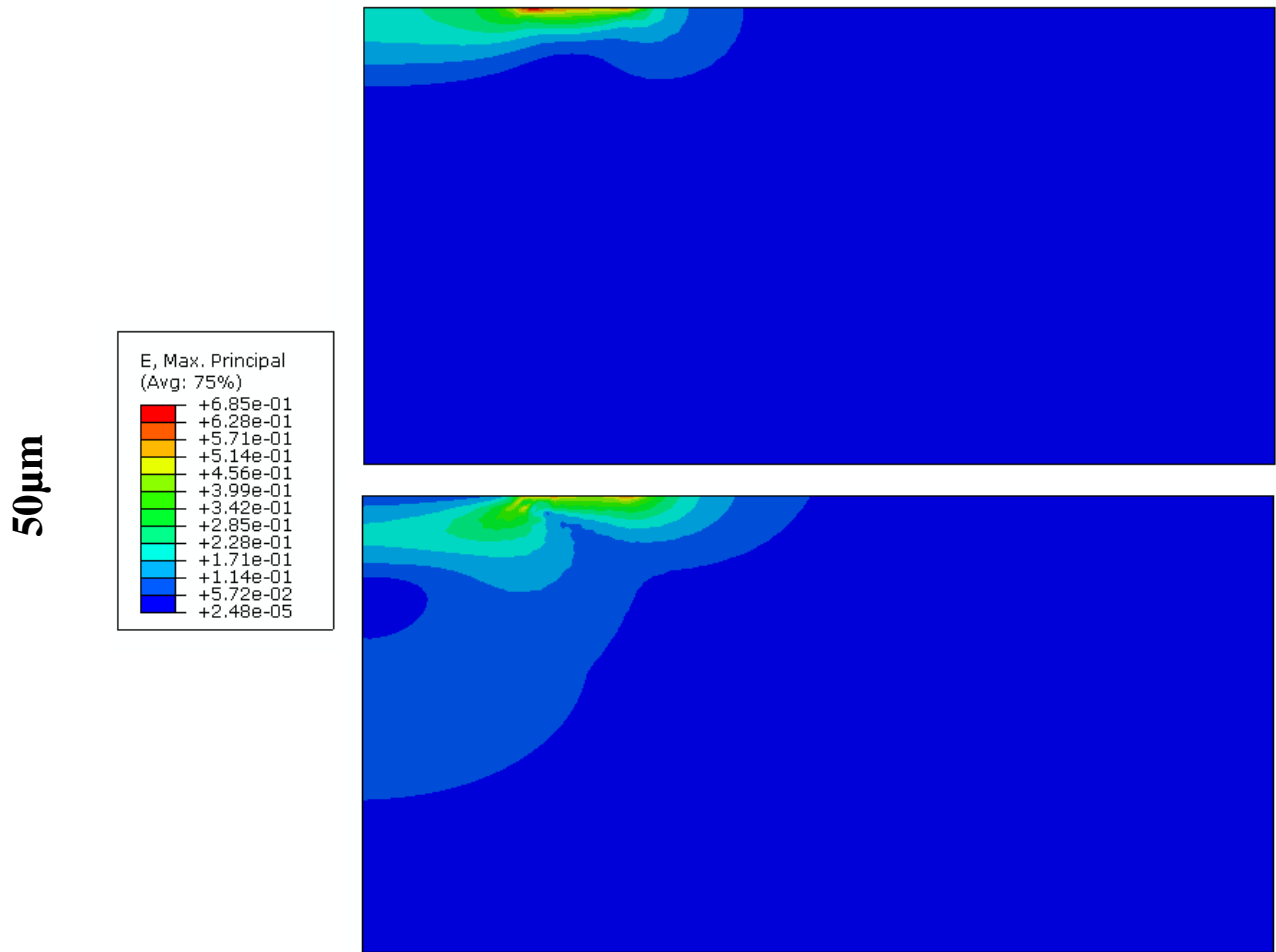


Fig. S10: Strain distributions for linear (above, 2kPa) and nonlinear (below, fibrin) gels of 1, 10, and 50 μm thickness, top to bottom with an applied traction of 500 Pa. The color scale is normalized to the maximum and minimum strains in each case to show the strain profiles regardless of magnitude (thus the plots for the other stiffness linear gels (not shown) have different magnitude but look identical). The strain profiles extend further into the strain-stiffening material compared to the linear material as can be seen by the lowest contour, representing roughly 9% of the maximum strain, “touching” the lower boundary in the 10 μm thick nonlinear gel but not in the linear gel.

Quantitative Comparison of Stress and Strain Distributions

From the above images of stress and strain contour plots of cell-applied traction on linear and nonlinear materials, we see that the stress in the nonlinear material does not travel as far as that in the linear material. In contrast, strains are transmitted further through the nonlinear than in the linear material.

For a quantitative comparison, two distances on the undeformed contour plots were measured for materials of “infinite” thickness (50 μm). The lateral distance from the outer point of the cell-applied traction to the farthest contour line was measured for strain and Von Mises stress for both materials. These variables were also quantified by measuring the vertical distance from the top surface to the farthest contour line along the axis of symmetry. This farthest contour line is the region where the variable is roughly 9% of the local maximum, representing stress or strain that has attenuated to that of the bulk material. The distances are shown in Table S2. Note the larger distance to the farthest strain

contour (strain extending) and the shorter distance to the farthest stress contour (stress blunting) of the nonlinear material compared to the linear material.

Table S2: Comparison of distances between the farthest contour line and either the outer edge of cell-applied traction (lateral) or symmetrical axis of the top surface (vertical)

		<i>Distance to farthest contour (μm)</i>	
		Linear (1kPa)	Nonlinear
Strain	<i>Lateral</i>	8.96	16.4
	<i>Vertical</i>	8.21	37.5
von Mises stress	<i>Lateral</i>	8.21	6.94
	<i>Vertical</i>	8.21	6.88

Changes in fiber alignment due to surface displacement in multi-scale model

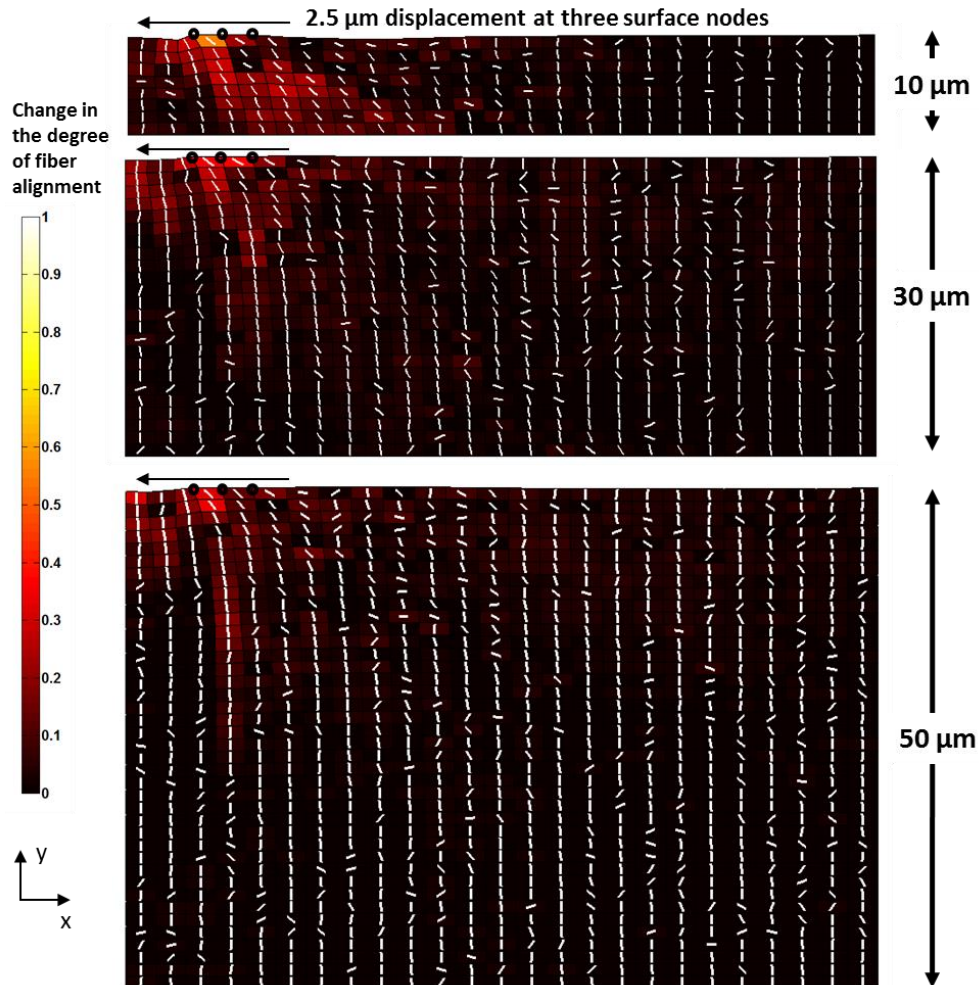


Fig. S11: Change in degree of fiber alignment (0-1 color scale) plots for the multi-scale models of 10 μm (top), 30 μm (middle), and 50 μm (bottom) thickness with fiber principal direction quivers (white) superimposed. The surface displacement causes noticeable reorganization of the fiber distributions approximately 15 μm into the 30 μm and 50 μm models, and more than 20 μm into the 10 μm model. The principal fiber directions remain relatively random far from the application of displacement.

Supporting References

1. Sen, S., A. J. Engler, and D. E. Discher. 2009. Matrix strains induced by cells: Computing how far cells can feel. *Cellular and Molecular Bioengineering* 2:39-48.
2. Mehrotra, S., S. C. Hunley, K. M. Pawelec, L. Zhang, I. Lee, S. Baek, and C. Chan. 2010. Cell adhesive behavior on thin polyelectrolyte multilayers: Cells attempt to achieve homeostasis of its adhesion energy. *Langmuir : the ACS Journal of Surfaces and Colloids* 26:12794-12802.
3. Munevar, S., Y. Wang, and M. Dembo. 2001. Traction force microscopy of migrating normal and H-ras transformed 3T3 fibroblasts. *Biophysical Journal* 80:1744-1757.
4. Winer, J. P., S. Oake, and P. A. Janmey. 2009. Non-linear elasticity of extracellular matrices enables contractile cells to communicate local position and orientation. *PLoS One* 4:e6382.
5. Yang, Z., J. S. Lin, J. Chen, and J. H. Wang. 2006. Determining substrate displacement and cell traction fields--a new approach. *Journal of Theoretical Biology* 242:607-616.
6. Hur, S. S., Y. Zhao, Y. S. Li, E. Botvinick, and S. Chien. 2009. Live Cells Exert 3-Dimensional Traction Forces on Their Substrata. *Cellular and Molecular Bioengineering* 2:425-436.
7. Engler, A. J., S. Sen, H. L. Sweeney, and D. E. Discher. 2006. Matrix elasticity directs stem cell lineage specification. *Cell* 126:677-689.
8. Solon, J., I. Levental, K. Sengupta, P. C. Georges, and P. A. Janmey. 2007. Fibroblast adaptation and stiffness matching to soft elastic substrates. *Biophysical Journal* 93:4453-4461.
9. Isenberg, B. C., P. A. Dimilla, M. Walker, S. Kim, and J. Y. Wong. 2009. Vascular smooth muscle cell durotaxis depends on substrate stiffness gradient strength. *Biophysical Journal* 97:1313-1322.